ORIGINAL PAPER

Strong hydraulic segmentation and leaf senescence due to dehydration may trigger die-back in *Nothofagus dombeyi* under severe droughts: a comparison with the co-occurring *Austrocedrus chilensis*

Fabián G. Scholz · Sandra J. Bucci · Guillermo Goldstein

Abstract

Key message **Total leaf hydraulic dysfunction during severe drought could lead to die-back in *N. dombeyi*, while hydraulic traits of *A. chilensis* allow it to operate far from the threshold of total hydraulic failure.**

Abstract Die-back was observed in South America temperate forests during one of the most severe droughts of the 20th century (1998–1999). During this drought *Austrocedrus chilensis* trees survived, whereas trees of the co-occurring species (*Nothofagus dombeyi*) experienced symptoms of water stress, such as leaf wilting and abscission, before tree die-back occurred. We compared hydraulic traits of these two species (a conifer and an angiosperm species, respectively) in a forest stand located close to the region with records of *N. dombeyi* mass mortality. We asked whether different hydraulic traits exhibited by the two species could help explain their contrasting survivorship rates. *Austrocedrus chilensis* had wide leaf safety margins, which appear to be the consequence of relatively high leaf-and-stem capacitance, large stored water use, strong stomatal control and ability to recover from embolism-induced loss of leaf hydraulic capacity. On the other hand, *N. dombeyi* even though had a stem hydraulic threshold of −6.7 MPa before reaching substantial hydraulic failure (P_{88}), leaf P_{88} occurred at leaf water potentials of only −2 MPa, which probably are reached during anomalous droughts. Massive mortality in *N. dombeyi* appears to be the result of the total loss of leaf hydraulic conductance leading to leaf dehydration and leaf drop. Drought occurs during the summer and it is highly likely that *N. dombeyi* cannot recover its photosynthetic surface to produce carbohydrates required to avoid tissue injury in the winter season with subfreezing temperatures. Strong hydraulic segmentation in *N. dombeyi* does not seem to have an adaptive value to survive severe droughts.

Keywords Capacitance · Leaf hydraulic conductance · P_{88} · Turgor loss point · Water storage

Communicated by A. C. Franco.

F. G. Scholz (✉) · S. J. Bucci · G. Goldstein
Consejo Nacional de Investigaciones Científicas y Técnicas (CONICET), Buenos Aires, Argentina
e-mail: fgscholz@yahoo.com

F. G. Scholz · S. J. Bucci
Grupo de Estudios Biofísicos y Eco-fisiológicos (GEBEF), Departamento de Biología, Facultad de Ciencias Naturales, Universidad Nacional de la Patagonia San Juan Bosco, Comodoro Rivadavia, Argentina

G. Goldstein
Laboratorio de Ecología Funcional (LEF), Departamento de Ecología, Genética y Evolución, FCEyN, Universidad de Buenos Aires, Buenos Aires, Argentina

Introduction

There is a large difference in hydraulic architecture traits between conifers and angiosperms resulting in a wide range in drought responses. Wood of conifers has only tracheids that are narrow and short, while angiosperms have mostly vessels and fibers of larger diameter and length than tracheids. These anatomical differences have ecophysiological correlations in terms of stomatal behavior, water stored use, resistance to cavitation, hydraulic safety margins and on the ability to refill embolized conduits, which may confer each group of plants a different behavior in relation to avoidance or tolerance to water deficits and potential inherent mortality risks (Gómez-

Aparicio et al. 2011; Carnicer et al. 2013; Coll et al. 2013). Although some conifers exhibit low stomatal conductance sensitivity to changes in air saturation deficits (ASD) (Johnson et al. 2011), other conifers may be more sensitive to ASD changes and close their stomata before embolism occur (Zwieniecki et al. 2007). A strong stomatal control of evaporative losses prevents leaves from reaching very negative water potentials (Ψ) which may contribute to larger hydraulic safety margins.

In water relation studies, knowledge of hydraulic safety margins is more informative that only documenting xylem Ψ because it indicates how close to the loss of its hydraulic capacity a plant operates. The safety margin is the difference between the lowest water potential experienced by e.g. leaves and a reference point at which certain amount of hydraulic dysfunction occurs in the xylem tissue. The xylem tension inducing 50 % loss of hydraulic conductance (P_{50}) is the most commonly used index of xylem embolism resistance to cavitation, however, this threshold value is not always an adequate reference point to compare the susceptibility to irreversible hydraulic failure across species. The value that better reflects the inherent risk to critical hydraulic failure appears to be the pressure inducing more than 88 % loss of hydraulic conductance (P_{88}) (Barigah et al. 2013; Urli et al. 2013) which represents the actual maximum species-specific tension experienced by most xylem conduits before becoming fully dysfunctional (Domec and Gartner 2001). Tissues (e.g. leaves and stems) of many species have not the ability to recover from 88 % loss of hydraulic conductivity while comparatively more vascular species can recover after reaching tensions inducing the 50 % loss of hydraulic conductivity (Blackman et al. 2009; Bodribb and Cochard 2009). These indices are weighted average behaviors of the vascular tissues because each tissue has an array of conduits with different susceptibility to cavitation. Although some conifers may be able to recover from drought-induced embolism (Zwieniecki and Holbrook 1998; Johnson et al. 2009), they are usually considered to have a relatively lower capacity to refill embolized xylem elements than angiosperms do (Brodribb et al. 2010). The P_{88} values not only differ between species, but also along the hydraulic continuum within the plants. In general, stems are less vulnerable to embolism than leaves (Pratt et al. 2007; Bucci et al. 2012, 2013; Hao et al. 2008; McCulloh et al. 2013) resulting in varying degrees of hydraulic segmentation (Tyree and Ewers 1991).

Although $\Psi_{min} - P_{50}$ safety margin can be small or negative in some species, a safety margin considering a higher hydraulic risk ($\Psi_{min} - P_{88}$) could better represent the ability of a plant to avoid death by irreversible hydraulic failure. Mechanisms such as capacitive water discharge in leaves or stems can reduce or slow down the water potential drop during a dry period (Bucci et al. 2008; Scholz et al. 2008). Some species from dry environments are vulnerable to hydraulic dysfunction but this low ability of the water transport pathway may be compensated by a large capacitance of the surrounding tissues (Barnard et al. 2011; Bucci et al. 2012).

Extensive tree mortality triggered by severe drought has been documented in forests worldwide (Allen et al. 2010). The precise mechanisms and plant traits underlying or mitigating species-specific mortality are poorly understood but they are currently the subject of a debate and ongoing research (McDowell et al. 2011; Allen et al. 2012; Choat et al. 2012; Sala et al. 2012; Hartmann et al. 2013; Plaut et al. 2013). Two mechanisms have been frequently suggested to explain drought-induced mortality in trees (McDowell et al. 2008). Species with a tight stomatal control to avoid hydraulic failure have a reduced CO_2 assimilation with consequences for its carbon economy eventually leading to carbon starvation (Sala et al. 2010; Adams et al. 2013). Anisohydric species (species with low stomatal control allowing large fluctuations in Ψ), however, are predisposed to hydraulic failure because they function with narrow hydraulic safety margins during dry periods (Bucci et al. 2013). Gymnosperms generally exhibit wider safety margins than angiosperms (Meinzer et al. 2009; Choat et al. 2012) but not always. While some conifer species in the Cupressaceae family survive extended drought periods, some *Pinaceae* species have very low resistance to embolism formation and safety margins resulting in widespread mortality events (Breshears et al. 2005). Selective mortality involving conifers and angiosperms has been observed in South America temperate forests during the 1998–1999 strong La Niña precipitation anomalies which led to a severe drought (Suarez et al. 2004). During this drought, *Austrocedrus chilensis* (Cupressaceae) trees survived whereas trees of the co-occurring angiosperm species (*Nothofagus dombeyi*; Nothofagaceae) experienced symptoms of water stress, such as leaf wilting and abscission before die-back occurred (Suarez et al. 2004).

In this study we compared several hydraulic traits of two dominant tree species in a mixed forest in the southern part of the Andes dominated by *A. chilensis* and *N. dombeyi*. We asked whether those different responses exhibited by these co-occurring gymnosperm and angiosperm species during one of the most severe drought of the 20th century in Patagonia could be explained by key hydraulic features other than differences in xylem anatomy. We expected that a higher hydraulic capacitance of the leaves and stem, stored water use and a higher capacity for embolism repair could mitigate the effects of severe droughts in *A. chilensis* while carbon starvation due to leaf shedding caused by a highly segmented hydraulic architecture can trigger die-

back in *N. dombeyi*. The implicit paradigm in this study is that the physiological underpinning of drought survival is a multi-dimensional problem and thus species-specific survival cannot be predicted with meaningful certainty by using a single parameter (e.g. stem P_{50}).

Materials and methods

The study was carried out in a site near Lago Puelo National Park, Chubut, Argentina ($42°05'01''$S; $71°37'28''$W) and approximately 70 km south of one of the sites indicated by Suarez et al. (2004) as having records of mass mortality in *N. dombeyi*. The study site has similar ecological characteristics compared to the ones that exhibited *N. dombeyi* die-back. The area has a mean annual precipitation of about 1,200 mm and a mean temperature of 11 °C. Precipitation is seasonally distributed with wet winters (June to September) and dry summers (December to March). Information from a site close to the study area (El Bolson city) indicates that accumulated precipitation during the previous 2 months (November and December) was only 32 mm and the air temperature was 14 °C, which is lower than the mean precipitation (close to 90 mm) and 2 °C higher to the mean air temperature for these months. The study site is a forest with abundant *A. chilensis* and *N. dombeyi* tree species. During January 2012 (the peak of the dry season) we selected 10 canopy trees per species with a mean DBH of 40.3 ± 3.8 cm in *A. chilensis* and 31.8 ± 2.58 cm in *N. dombeyi* to perform the physiological measurements. Both species were sampled on the same days.

Austrocedrus chilensis (D.Don) Pic. Sern. et Bizarri is an endemic conifer species of the temperate sub-antarctic forests of Patagonia and grows up to 1000 m.a.s.l., in habitats with more than 2000 mm to less than 400 mm rainfall and from $36°30'$S to $43°35'$S. This species only grows with shrubs and grasses in the driest sites and with *N. dombeyi* (Mirsb) Oerst in relatively wet sites. Mortality of *A. chilensis* has been reported since the last half of the 20th century throughout its range of distribution. Mortality of *A. chilensis* is locally known as "mal del cipres" (cypress sickness) and it is associated with biotic factors such as Phytophthora species (Greslebin et al. 2005) and with poorly drained soils (La Manna and Rajchenberg 2004).

Nothofagus dombeyi is one of the nine species of Nothofagus occurring in South America. It is an evergreen species growing between 39 and 45°S and with an altitudinal range of 400–1,200 m a.s.l. There are nine Nothofagus species in southern Argentina and Chile with only three of them being evergreen: *N. dombeyi*, *N. betuloides* and *N. nitida*. All other Nothofagus species are deciduous.

In mixed forest with *A. chilensis*, *N. dombeyi* exhibited larger mortality than *A. chilensis* under severe droughts (57 and 5 %, respectively; Suarez and Kitzberger 2008).

Leaf water potential and leaf pressure–volume relationships

Predawn and minimum leaf water potentials were measured with a pressure chamber (PMS; Albany, Oregon) during January 2012. Leaf water potentials of ten small leafy twigs from different individuals per species ($n = 10$) were measured before dawn and at 12 h. We used leafy twigs instead of leaves because the petioles are very short.

The pressure–volume (P–V) relationships of small leafy twigs were developed by the dehydration technique to estimate bulk leaf water relations for each species. Measurements were performed on exposed, expanded terminal twigs. Five leafy twigs per species (one twig per tree; $n = 5$) were sampled at predawn. The leafy twigs were first weighed to the nearest 0.001 mg to obtain the initial fresh mass and immediately placed in the pressure chamber (PMS system, Corvallis) to obtain the initial water potential. The procedure was repeated many times while the leafy twig was allowed to slowly dehydrate under laboratory conditions (20–25 °C). Finally, the twigs were dried in a force-convection oven at 80 °C for 72 h and their dry mass was recorded. Saturated mass of non-hydrated samples was estimated by determining hydrated/dry mass ratios from parallel samples obtained from the same individual on the same date. The tissue water relation parameters calculated from P–V relationships were water potential at the turgor loss point (Ψ_{TLP}) and leaf capacitance (C_{leaf}). Leaf capacitance values (mol m^{-2} MPa^{-1}) were determined from slopes of cumulative mass of water released per leaf area (mol m^{-2}) against leaf water potential (MPa).

Leaf hydraulic vulnerability

Leaf hydraulic vulnerability curves were determined by measuring leaf hydraulic conductance (K_{leaf} mmol m^{-2} s^{-1} MPa^{-1}) from small leafy twigs collected from ten different trees per species using the partial rehydration method described by Brodribb and Holbrook (2003). The measurement is based on the analogy between rehydration of partially desiccated leaves and charging of a capacitor through a resistor as follows:

$$K_{leaf} = C_{leaf} \ln(\psi_o/\psi_f)/t$$

where C_{leaf} is leaf capacitance, Ψ_0 is leaf water potential before rehydration, and Ψ_f is leaf water potential after rehydration for t seconds. A range of leaf Ψ measured on leafy twigs was attained through slow bench dehydration of

large branches of ten trees per species collected from the field. Some samples were previously hydrated for 1 or 2 h to obtain leaf Ψ close to zero. Leaf water potentials for K_{leaf} calculations were then measured after 0.5–1 h equilibration (depending of the dehydration degree) inside black plastic bags with slightly humid paper towels. Leaf vulnerability curves were plotted as loss of K_{leaf} (%) against initial leaf Ψ before rehydration. Leaf P_{50} and P_{88} values were obtained from sigmoid functions fitted to the data at water potential at which the 50 and 88 % of loss of K_{leaf} occur, respectively. The leaf hydraulic conductance was also measured in leafy twigs collected at predawn, mid-morning, midday, 15 and 18 h.

Stem xylem vulnerability

Hydraulic vulnerability was determined on stems from 5 to 7 individuals per species by plotting the percent loss of hydraulic conductivity (PLC) against stem Ψ. Different PLC values were obtained by allowing large branches excised in the early morning to dehydrate slowly in air for different time periods (Tyree and Sperry 1989). After allowing time for partial dehydration, branches were placed in sealable bags with a wet paper towel. After equilibration for at least 30 min (depending of the dehydration degree) measurements of Ψ from non-transpiring small leafy twigs and hydraulic conductivity (k_{h}) of a stem segment were obtained for each branch. The stem Ψ and leaf Ψ were assumed to be in equilibrium because the branches were slowly dehydrated. Maximum hydraulic conductivity (k_{hmax}) was obtained by flushing the samples with filtered water at a pressure of 0.2 MPa for 15 min to remove air bubbles from embolized vessels. Percent loss of hydraulic conductivity was calculated as:

$$\mathrm{PLC} = 100 \times \left(1 - \frac{k_{\mathrm{h}}}{k_{\mathrm{hmax}}}\right)$$

To measure k_{h}, the underwater cut ends of stem segments were attached to the hydraulic conductivity apparatus (Tyree and Sperry 1989). Distilled water was used as the perfusion fluid. Relatively low hydrostatic pressure generated by a constant hydraulic head of 50 cm was applied to avoid refilling of embolized vessels. Hydraulic conductivity (kg m s^{-1} MPa^{-1}) was calculated as the ratio of the flow rate through the segment (J_{v} kg s^{-1}) and the pressure gradient across the segment ($\Delta P/\Delta L$ MPa m^{-1}). Stem P_{50} and P_{88} values were obtained from sigmoid functions fitted to the data at water potential at which the 50 and 88 % of k_{h} loss occurs, respectively. Sapwood and leaf specific hydraulic conductivity were obtained by dividing k$_{\mathrm{h}}$ by the cross sectional active xylem area and by the total projected leaf area distal to the stem segment, respectively. Sampling methods may generate artifacts in

PLC patterns inducing a certain degree of embolism that is itself a function of xylem tensions at the moment of sample excision (Wheeler et al. 2013). The artifacts could be introduced during excision. In our study, the branches were excised at dawn when water potentials were high, thus minimizing the risk of artifacts in PLC determinations.

Sapwood density and capacitance

Wood density (ρ) was measured by the water-displacement method on samples collected from the trunk of ten trees per species (one sample per tree). Each sample of sapwood was obtained with a 5 mm increment borer and sealed in glass vials to be transported to the laboratory. After removal of bark and pith, ρ (g cm^{-3})was calculated as:

$$\rho = \frac{M}{V}$$

where M is the dry mass of the sample (oven dried at 60 °C for 72 h) and V is the sample volume. Volume was estimated by submerging the sample in a container with distilled water resting on a digital balance with a 0.001 g precision. The sample was kept submerged during measurements with the help of a very small needle, without touching the walls of the container. Saturated water content was determined dividing the saturated mass minus dry mass by the dry mass.

To determine sapwood capacitance, cylinders of sapwood were obtained with a 5 mm increment borer in the trunk of three trees per species and sealed in glass vials. These samples were transported to the laboratory where they were allowed to hydrate in distilled water for <2 h to avoid oversaturation, quickly blotted to remove excess water, placed in the caps of thermocouple psychrometer chambers (JRD Merrill Specialty Equipment, Logan, UT, USA), weighed, and then sealed inside the chamber for determination of water potential isotherms. Each chamber contained three cylindrical tissue samples. The psychrometer chambers were placed in an insulated water bath and allowed to equilibrate for at least 3 h before measurements with a dew point micro-voltmeter (HR-33T, Wescor, Logan, UT, USA). Measurements were repeated at frequent intervals until the water potential values stabilized. The chambers were then opened and the samples allowed dehydrating for different time intervals, re-weighed in the chamber caps, resealed inside the psychrometer chambers and allowed to equilibrate for another determination of water potentials. Moisture release curves were generated by plotting water potential against relative water content. Curves fitted to the relationships between sapwood water potential and relative water content were used to calculate sapwood capacitance as described in Meinzer et al. (2003). Capacitance was normalized by the sapwood tissue volume

to facilitate comparison of absolute amounts of water released per unit decline in water potential. Sapwood capacitance (kg m^{-3} MPa^{-1}) was calculated as:

$$\text{Sapwood capacitance} = \frac{\partial W}{\partial \varphi}$$

Where W is mass of water per unit volume of tissue and φ is the water potential of the tissue. Mass of water per unit tissue volume at saturation (kg m^{-3}) was calculated by multiplying the saturated/dry mass ratio of each tissue by tissue density (kg m^{-3}) and subtracting tissue density. The cumulative mass of water released per unit tissue volume was then calculated by multiplying the tissue relative water deficit (1-RWC) at a given value of tissue water potential by the mass of water per unit tissue volume at saturation. Capacitance values were determined from instantaneous slopes of plots of cumulative mass of water released against tissue water potential. Species-specific values of tissue capacitance were calculated as the slope of linear regressions fitted to the initial phase of each water release curve. Although this method could not reflect the capacitance in the operating range of each species (Richards et al. 2013), for the study species the minimum water potentials were close to the inflection point in the curve and both species exhibited a similar native operating range ($\Delta\Psi$) within the initial linear portion of the water release curve. We do not know the Ψ these species experience during drier conditions, which probably lay on the flatter portion of the release curve, leading to a different value of capacitance than the capacitance obtained using their actual operational range.

Sap flow and stem water storage calculations

Sap flow in *A. chilensis* was measured with the heat-dissipation method (Granier 1985, 1987) in three individuals with mean DBH of 33.3 ± 2.35 cm during the summer of 2012. Briefly, a pair of 20 mm long, 2 mm diameter hypodermic needles containing a copper-constantan thermocouple inside a glass capillary tube and a heating element of constantan coiled around the glass tube was inserted into the sapwood near the base of the main trunk and on a second-order branch (near the tree top). Both probes were installed in the same azimuthal position. The upper (downstream) probe was continuously heated at a constant power by the Joule effect, while the unheated upstream probe served as a temperature reference. Temperature differences between the upstream and downstream probes were recorded every 10 sec and 10 min averages were stored in data loggers (CR 1000, Campbell Scientific). Sap flux density was calculated from the temperature difference between the two probes using an empirical calibration (Granier 1985, 1987). The measured temperature

differences between both probes were corrected for natural temperature gradients between the probes (Do and Rocheteau 2002). The probes were left in the tree for few days to avoid or minimize wound effects. Mass flow of sap per individual was obtained by multiplying flux density by the active sapwood cross-sectional area. The sapwood cross-sectional area was obtained by injecting dye near the base of the main trunk and in a branch per tree for several trees of each species representing a range of diameters. After 2 h cylinders of sapwood were obtained with a 5 mm increment borer and determined by the portion dyed.

Branch sap flow rates were used to obtain whole-crown transpiration according to Goldstein et al. (1998). Whole-crown transpiration was estimated by normalizing branch sap flow with respect to the average daily maximum value. Normalized branch sap flow was then divided by the daily sum of the normalized 10 min averages divided by 6, then multiplied by the total daily sap flow measured at the base of the tree which was assumed to be equal to total daily transpiration according to the principle of conservation of mass. This procedure yielded estimated rates of crown transpiration on an hourly basis. Total diurnal stem water storage capacity was estimated by subtracting 10 min averages of basal sap flow from whole crown sap flow when basal sap flow was less than whole-crown flow, summing the differences, then dividing by six. It was not possible to collect data for *N. dombeyi* due to technical problems with one of the dataloggers.

Stem diameter changes

Electronic dendrometers (models DEX70 and DEX100, Dynamax Inc. Houston, TX, USA) were installed in the trunk of the same three trees used to determine sap flow in *A. chilensis*. Dendrometers were placed in an intermediate position between both sap flow sensors. To monitor whole-stem diameter fluctuations, the bark was smoothed before dendrometer attachment and then covered with rubber foam insulation and aluminum foil to minimize heating by direct solar radiation. To monitor sapwood diameter fluctuations, the sapwood surface was exposed by removing the outer parenchyma (cortex) from two small areas on opposite sides of the stem. Data were obtained every 10 s, and 10 min averages were recorded with a data logger (CR1000, Campbell Scientific), taking the signals from the full-bridge strain gage attached to the flexible frame of the caliper-style dendrometers. The frame temperature was measured with copper-constantan thermocouples to correct for potential temperature effects on the dendrometer frame. To estimate the temperature correction factor, dendrometers were also installed on cut stems with the ends sealed and the whole stem wrapped in aluminum foil to prevent water loss. These stem sections with the dendrometers were

placed next to the dendrometers used on intact stems to insure similar temperature and light conditions. The temperature correction factor was 0.046 mm per 20 °C, similar to the temperature correction specified by the manufacturer. We have no data of stem diameter changes in *N. dombeyi* due to the same data logger failure used to measure sap flow in this species.

Statistical analysis

The SPSS 11.5 statistical package (SPSS Inc., Chicago, IL, USA) was used for statistical analysis. A one-way analysis of variance (ANOVA) was used to test for differences in leaf water potentials (predawn, midday and TLP) within each species. To test for differences in one variable between species, a student test was performed.

Sigma plot version 11 (Systat Software, Inc., Chicago, IL, USA) was used to fit functions for all vulnerability curves. Vulnerability curves were fitted to the data with three-parameter sigmoidal functions, but a Weibull function was fitted to leaf vulnerability curve in *A. chilensis*. Linear functions were fitted to water release curves. The slopes of water release curves were compared with an analysis of covariance (ANCOVA).

Results

During the hottest and driest month of the year (January). the predawn and midday leaf water potentials (Ψ) were similar between species (Fig. 1). While predawn $\Psi \times \Psi_{max}$ was approximately −0.5 MPa, midday $\Psi \times \Psi_{min}$ was −1.4 MPa for both species. However, the Ψ at turgor loss point Ψ_{TLP}) was significantly higher (less negative) in *A. chilensis* (−1.1 MPa) than in *N. dombeyi* (−1.63 MPa). In *A. chilensis* leaf Ψ_{min} was more negative than leaf Ψ_{TLP} (Fig. 1).

Leaf and stem vulnerability curves differed between species (Fig. 2). The water potential at which leaves lose 50 % of its hydraulic conductance (leaf P_{50}) was higher in *A. chilensis* than in *N. dombeyi*; nevertheless this behavior was opposite when it was considered the leaf water potential at which leaves lose 88 % of its maximum hydraulic conductance (P_{88}) (Fig. 2 a, c). Leaf P_{88} in *A. chilensis* was −3.0 MPa while in *N. dombeyi* leaf P_{88} was −2.0 MPa. At stem level, both stem P_{50} and P_{88} were about 2 MPa more negative in *N. dombeyi* compared to *A. chilensis* (Fig. 2 b, d) and lower than in the leaves for both species. *Nothofagus dombeyi* exhibited larger differences between leaf P_{88} and stem P_{88} (4.7 MPa) compared to *A. chilensis* (1.4 MPa) (Fig. 2; Table 1). The leaf hydraulic safety margin estimated as Ψ_{min}–P_{50} was negative for *A.*
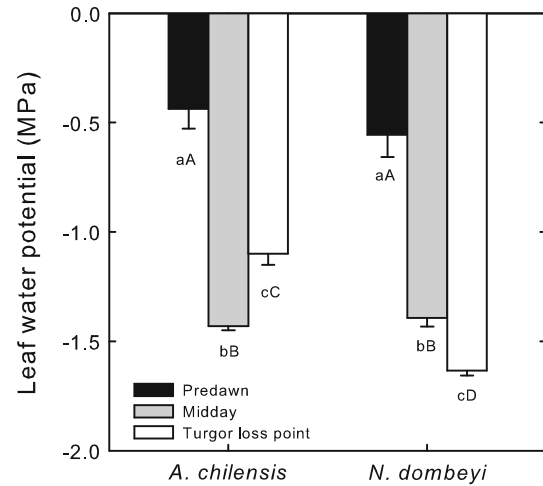

Fig. 1 Leaf water potentials at predawn (*filled bars*), midday (*gray bars*) and at the turgor loss point (*open bars*) in *A. chilensis* and *N. dombeyi* during the peak of the dry season (summer). Each *bar* represents the mean value–1SE ($n = 10$ for predawn and midday leaf water potential and $n = 5$ for turgor loss point). Different lower case letters between bars indicate significant differences between leaf water potentials within species (One-way ANOVA; $p < 0.05$). Different capital letters indicate significant differences in leaf water potential between species (student test; $p < 0.05$)

chilensis and close to zero for *N. dombeyi* (Fig. 3). Other leaf hydraulic safety margins using P_{88} as a reference point (Ψ_{min}–P_{88}, Ψ_{TLP}–P_{88}, and P_{50}–P_{88}) were always positive and two to four times higher in *A. chilensis* than in *N. dombeyi* (Fig. 3; Table 1).

Leaf hydraulic conductance (K_{leaf}) varied during the daytime in both species but the K_{leaf} of *A. chilensis* was always higher than K_{leaf} of *N. dombeyi* (Fig. 4). Leaf hydraulic conductance was higher in the morning and significantly lower near midday and then recovered in the afternoon in both species, but the magnitude of the diurnal fluctuations was substantially larger in *A. chilensis*. The K_{leaf} in *A. chilensis* varied between 56.2 and 27 mol m^{-2} s^{-1} MPa^{-1}, while in *N. dombeyi* varied between 17 and 11 mol m^{-2} s^{-1} MPa^{-1}. In *N. dombeyi* native K_{leaf} (measured at predawn) was substantially lower than maximum K_{leaf} (measured from rehydrated leaves at Ψ close to zero MPa) (22 % lower), however, in *A. chilensis* native and maximum K_{leaf} were similar (Fig. 4).

The rate of decline of normalized water release on a leaf area basis as a function of leaf Ψ, an estimate of leaf capacitance (C_{leaf}), was higher for *A. chilensis* compared to *N. dombeyi*, both before and after turgor loss point (Fig. 5). Slopes were statistically different ($P = 0.0001$) between species, before and after turgor loss point. Leaf capacitance for *A. chilensis* was more than twofold higher than C_{leaf} in *N. dombeyi*. Both species exhibited higher C_{leaf} after turgor loss point (Fig. 5).
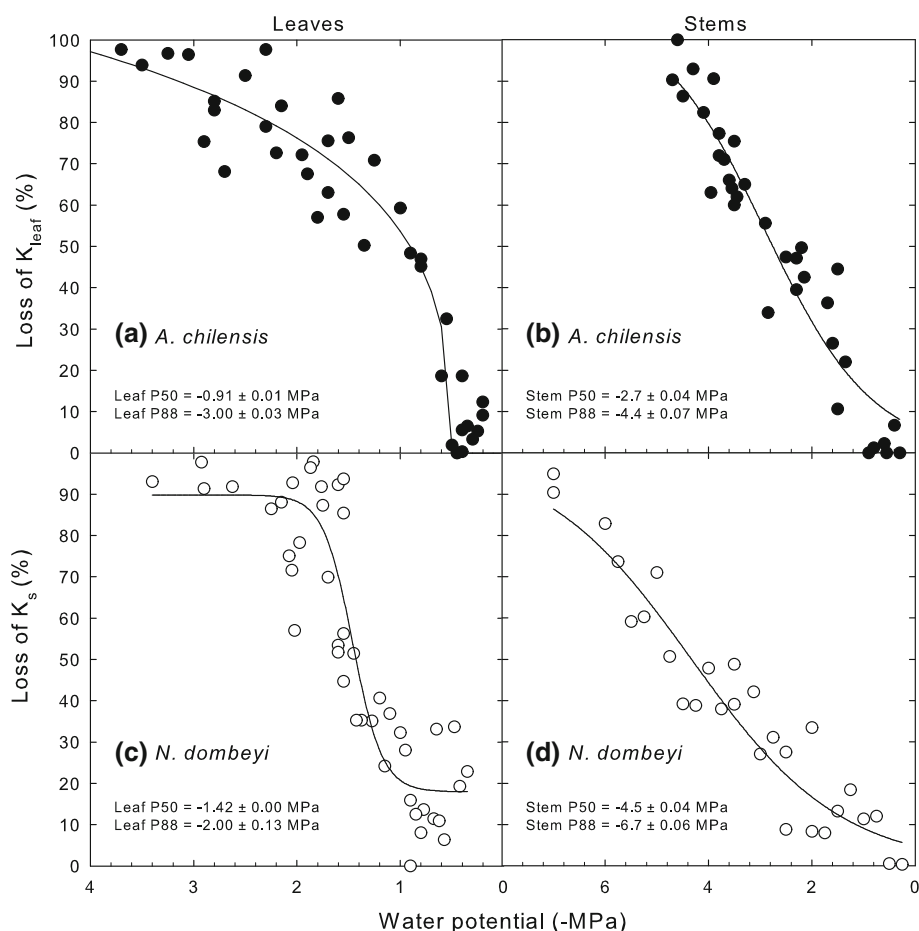
Fig. 2 Leaf and stem vulnerability curves of *A. chilensis* (**a**, **b**) and *N. dombeyi* (**c**, **d**). The water potential at the 50 % loss of leaf and stem hydraulic conductance (leaf P_{50} and stem P_{50}) and the water potential at the 88 % loss of leaf and stem hydraulic conductance (leaf P_{88} and stem $P_{88} \pm$ SE) are indicated in each panel. Leaf and stem vulnerability were best described by:

$$\mathbf{a}\ y = 185 \left(1 - e^{\left(-\left(\frac{x-3.4+7.4\times\ln(2)^{\frac{1}{0.39}}}{7.4} \right)^{0.39} \right)} \right), \mathbf{b}\ y = \frac{93.4}{1+e^{\frac{-x-1.3}{0.4}}};$$

$$\mathbf{c}\ y = 17.946 + 71.88\left(1 + e\left(-\frac{x-1.46}{0.1431}\right)\right), \mathbf{d}\ y = \frac{120.1}{1-\frac{e^{x-5.1}}{1.7}}$$

Sapwood density was significantly lower in *A. chilensis* than in *N. dombeyi* while saturated water content and sapwood capacitance had an opposite behavior (Table 1). Sapwood-specific and leaf-specific hydraulic conductivity was higher in *A. chilensis* than in *N. dombeyi*, however the differences were not significant (Table 1).
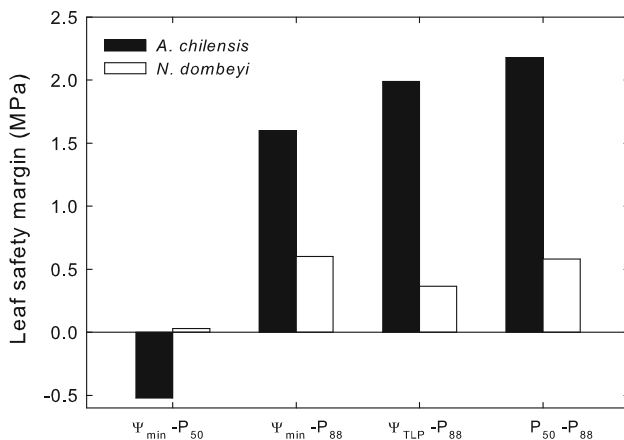
Sap flow in *A. chilensis* increased earlier in branches than at the base of the trunk in the early morning with a lag of about 1 h (Fig. 6a). Additionally, the maximum sap flow is reached sooner in the crown than at the base of the main stem. While the maximum sap flow in branches occurred at midday, at the base of the tree it was reached at 21 h for both days of measurements. Differences in the time course of the basal sap flow and crown sap flow were used to determine periods of discharge and recharge of water from internal stem storages (Fig. 6b). The discharge of water from internal

water storage occurred between 7 and 18 h (positive values of crown –basal sap flow) and the recharge occurred at nighttime (Fig. 6b). The mean total water use per day for *A. chilensis* trees was approximately 40 l, of which 7.7l day^{-1} were derived from stem water storages. Consistent with the discharge and recharge of stem water storages, daily variations in stem diameter both in the sapwood as well as in the cortex were observed (Fig. 6c). Increases in stem diameters indicate that water from the soil was recharging the stem storages, while decreasing values indicate that the stem diameter was being reduced as a consequence of the discharge of water from storages. The changes at initial contraction and at final expansion of both tissues (sapwood and total stem) were similar but after midday and up to 22 h the changes in total stem diameter were larger than in the sapwood (Fig. 6c).

Table 1 Wood density, wood saturated water content and capacitance in the main trunk, sapwood specific and leaf specific hydraulic conductivity of terminal branches and hydraulic safety margins (leaf Ψ_{min} − leaf P_{88} and leaf P_{88} − stem P_{88}) in *A. chilensis* and *N. dombeyi*

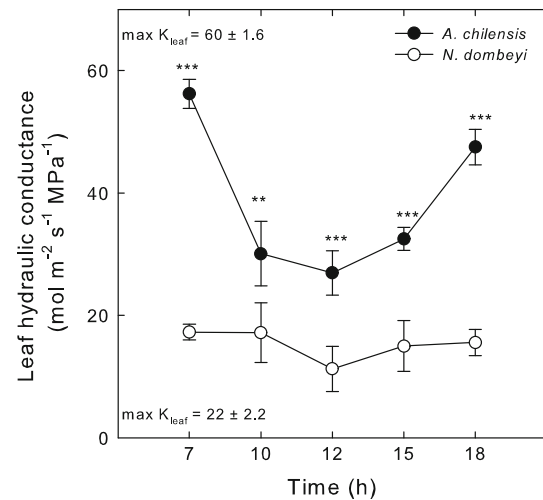|	A. chilensis	N. dombeyi
Wood density (g cm^{-3}) ($n = 10$)	0.50 ± 0.01^a	0.54 ± 0.02^b
Wood saturated water content (%) ($n = 10$)	130 ± 4.6^a	91 ± 3.8^b
Sapwood capacitance (kg m^{-3} s$^-$ MPa^{-1}) ($n = 3$)	375 ± 32^a	178 ± 14^b
Sapwood specific hydraulic conductivity (kg m^{-1} s^{-1} MPa^{-1}) ($n = 5$–7)	0.84 ± 0.06	0.65 ± 0.09
Leaf specific hydraulic conductivity ($\times 10^{-4}$ kg m^{-1} s^{-1} MPa^{-1}) ($n = 5$–7)	5.1 ± 0.96	4.3 ± 1.1
Leaf Ψ_{min} − leaf P_{88} (MPa)	1.6 ± 0.05	0.6 ± 0.04
Leaf P_{88} − stem P_{88} (MPa)	1.4 ± 0.1	4.7 ± 0.19

We have done error propagation as additive for safety margins and have estimated the standard error for the other parameters. Different letters indicate significant differences between columns ($p < 0.05$)

Fig. 4 Diurnal variations in leaf hydraulic conductance (K_{leaf}) in *A. chilensis* (*filled symbols*) and in *N. dombeyi* (*open symbols*) during the dry season. Each point is the mean value ± SE for ten leaves per species. ***Significant difference between species at $p < 0.001$. The maximum K_{leaf} values measured at water potential close to zero MPa are indicated in each panel

Fig. 3 Leaf safety margins between **a** midday leaf water potential and water potential at the 50 % loss of leaf hydraulic conductance ($\Psi_{min} - P_{50}$), **b** Ψ_{min} and water potential at the 88 % loss of leaf hydraulic conductance ($\Psi_{min} - P_{88}$), **c** water potential at the turgor loss point and P_{88} ($\Psi_{TLP} - P_{88}$) and **d** $P_{50} - P_{88}$ for leaves of *A. chilensis* (*filled bars*) and *N. dombeyi* (*open bars*)

Discussion

This study investigated possible physiological mechanisms responsible for the observed die-back in *N. dombeyi* during a severe drought in 1998–1999, while it also contributes to understand why the co-occurring conifer, *A. chilensis*, survived. These species specific plant traits observed in this study also help to explain their patterns of ecological distribution along the Andean forests, with *A. chilensis* reaching the xeric portion of the Andean forests in the ecotone with the patagonian steppe, and *N. dombeyi* growth restricted to relatively wet habitats. Dendrocronological studies of forests in the eastern limit of *N. dombeyi* distribution (xeric boundary for this species) had indicated that drought and heat events induce instantaneous as well as lagged tree mortality effects in *N. dombeyi* (Suarez and Kizberger 2010). Records of mortality of *N. dombeyi* in these more xeric forests, however, were not associated to climatic events causing mechanical damage (strong wind and snowfalls). For *A. chilensis*, records of erratic mortality throughout the natural range of the distribution, have been observed perhaps as a result of complex interaction between biotic (e.g. *Phytophthora austrocedrae*) and abiotic factors (e.g. poorly drained soils) more than by extreme drought per se (Greslebin et al. 2005; Mundo et al. 2010). Blockage of xylem conduits by hyphal colonization in *P. austrocedrae* vascular tissues results in a loss of hydraulic conductivity (Velez et al. 2012), similar to the effects of drought.

Vulnerability of leaves and stems to cavitation

Resistance of the water transport system in plants is estimated according to certain levels of embolism formation. Pressures inducing 50 and 88 % of embolism formation (P_{50} and P_{88}) are indexes commonly used to evaluate drought stress effects in plants, however, the value better reflecting the inherent risk of critical hydraulic failure in the study species is the pressure resulting in 88 % loss of leaf hydraulic conductance. Although angiosperm plants death may occur at water potential well beyond the leaf
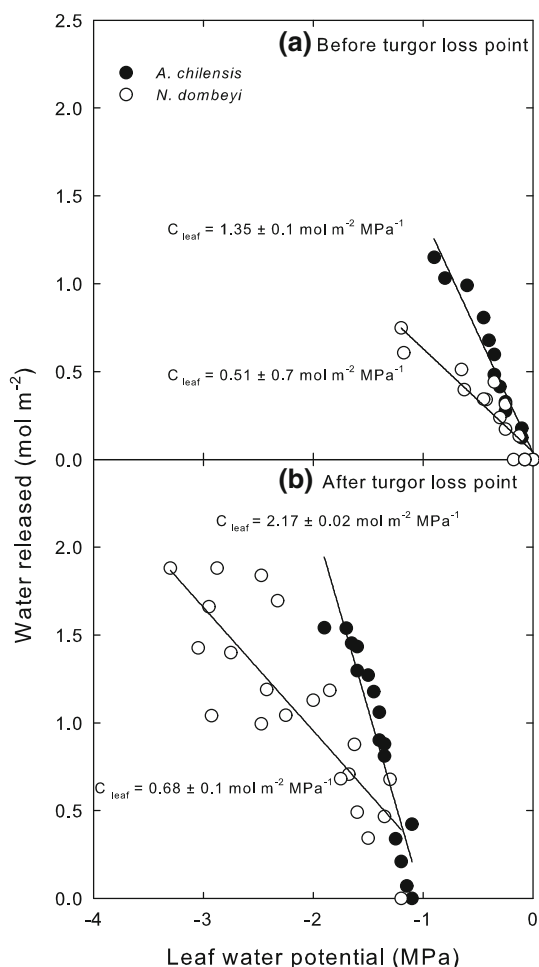
Fig. 5 Leaf water release as a function of the water potential **a** before turgor loss point (TLP) and **b** after TLP in *A. chilensis* (*filled symbols*) and *N. dombeyi* (*open symbols*). The *lines* are the linear regressions fitted to the data **a** $R^2 = 0.93$, $p < 0.001$ and $R^2 = 0.86$, $p < 0.001$, **b** $R^2 = 0.87$, $p < 0.001$; $R^2 = 0.72$, $p < 0.001$). For each species the leaf capacitance value $\pm$ SE (C_{leaf}; mol m^{-2} s^{-1} MPa^{-1}) is indicated which was obtained by the slope between leaf water released and water potential. In **b** water released was calculated from TLP which was considered as zero at that point

P_{88}, which is associated with massive stem or total hydraulic failure (Blackman et al. 2009; Barigah et al. 2013; Urli et al. 2013), *N. dombeyi* had stems with safety margins higher than 5 MPa before reaching stem P_{88}; thus the probability of this species achieving high levels of embolisms in stems is low even under extreme drought conditions. On the other hand, the leaf P_{88} occurred at water potentials of -2 MPa that probably are frequently reached during anomalous droughts. We hypothesized that massive mortality observed in *N. dombeyi* is the consequence of strong hydraulic segmentation and thus the total loss of K_{leaf} which triggers leaf senescence and leaf drop.
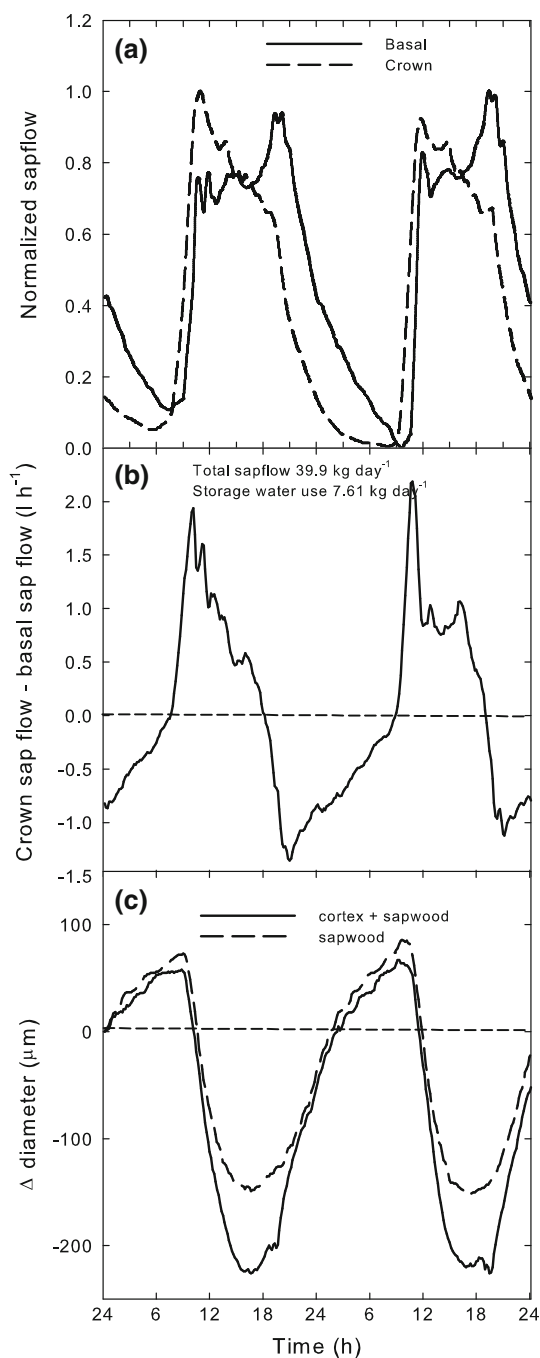
Fig. 6 Typical daily courses of **a** sap flow in the crown and near the base of the trunk for *A. chilensis* normalized by its maximum value, **b** daily difference between crown and basal sap flow, **c** changes in the stem diameter (Δ diameter) considering cortex and sapwood (*solid line*) and only sapwood (*dashed line*) in *A. chilensis* during the 14 and 15 January 2012. Positive values of the difference between crown and basal sap flow indicate time periods when water transpired was principally discharged from the stem water storage, and negative values indicate time periods when water from the soil was refilling water storage. Positive values of Δ diameter indicate stem expansion and negative values indicate stem contraction

Droughts occur during the summer (December–March) and it is highly likely that *N. dombeyi* trees cannot recover its photosynthetic leaf surface before the beginning of the cold seasons (autumn and winter) when the air temperatures drop below freezing. *Nothofagus dombeyi* is one of the three evergreen species in the South America Nothofagus genus and requires high levels of available carbohydrates during winter to enhance its freezing tolerance (Alberdi 1987; Reyes-Díaz et al. 2005), either through their protective role on membrane stabilization or by their effects on freezing point depression. Consequently, if the lack of CO_2 assimilation restricts carbohydrate production before and during winter, damage of active stem and root tissues may occur as a result of carbon starvation. Studies on *Nothofagus* species indicate that while deciduous species produce and store non-structural carbohydrates before leaves fall to maintain the plant metabolism during the period without leaves, evergreen species such as *N. dombeyi* depends on the continue production of carbohydrates to cope with low temperatures as their tissues store small amounts of non-structural carbohydrates (Riveros et al. 2003; Fajardo et al. 2013). Depletion of carbon reserve and production as the result of drought-induced defoliation had been recently observed in P*inus* P*alustris* (Poyatos et al. 2013). Future studies on *N. dombeyi* should consider measuring carbon availability after drought stress and their subsequent response to low temperatures.

The higher loss of hydraulic capacity at low water potentials in *N. dombeyi* can have a positive feedback due to water released via cavitation, which can play a significant buffering effect in xylem water relations on a short time basis (Meinzer et al. 2009; Scholz et al. 2011). This could be advantageous in species with high capacity to recover K_{leaf} on daily basis; however, the low native K_{leaf} (22.8 % lower than max K_{leaf}) observed in *N. dombeyi* suggests that conduit refilling is limited perhaps due to high carbon costs associated with this process (Bucci et al. 2003; Zwieniecki and Holbrook 2009; Nardini et al. 2011). Under extended and severe droughts K_{leaf} may drop to substantially low values resulting in leaf senescence and eventually to plant death. The loss of K_{leaf} due to strong hydraulic segmentation during water stress may have both positive (e.g. releasing water to the transpiration stream) and negative (e.g. leaf death) impacts, and these impacts need to be carefully considered if we want to understand more broadly the fitness benefits of these hydraulic traits.

In an experimental study where four conifer species from wet and dry forests were exposed to different levels of water stress by withholding water followed by re-watering, the death of stressed plants was observed at water potentials close to 95 % loss of K_{leaf} (Brodribb and Cochard 2009). In our study, *A. chilensis* operated under water potentials far from P_{88}, with leaf hydraulic safety margins

(using P_{88}) being always positive and two–four times higher than those observed in *N. dombeyi*. Larger values of these safety margins indicate a more gradual loss of leaf hydraulic conductance as the water potential drops from TLP or P_{50} down to P_{88} where leaf hydraulic failure is almost complete. Total loss of hydraulic conductance both in leaves and stems is unlikely to occur in *A. chilensis* during long droughts.

Very low stem P_{88} values in *N. dombeyi* are not directly related to drought resistance because the hydraulic bottleneck seems to be in the leaves. *Nothofagus dombeyi* exhibited a strong hydraulic segmentation between leaves and stems compared to *A. chilensis* (4.7 and 1.4 MPa, respectively). Drought stress triggers a nonlinear, spatio-temporal dynamics within the hydraulic network of trees, which may lead to a breakdown of the hydraulic system (Tyree and Ewers, 1991); it is more likely that this phenomenon occurs in *N. dombeyi* than in *A. chilensis* because their leaves exhibit higher leaf P_{88}. In dry sites where both species are co dominant, drought is the main factor affecting the demography of *N. dombeyi*, however, in the rain forests on the western slopes of the Andes where *N. dombeyi* is dominant, climatic-induced mechanical disturbance (snow and wind) prevails as disturbance mechanism (Suarez and Kitzberger 2010). The stem P_{88} threshold for *N. dombeyi* was −6.7 MPa probably as consequence of its higher wood density, which could provide mechanical resistance and/or to reduce maintenance cost per mass unit (Larjavaara and Muller-Landau 2010). Denser wood can be the result of narrow conduits, fibers or/and thick-walled conduits which can contribute to tolerance of high tensions or to protect conduits from implosion.(Hacke et al. 2001). Previously, we found a linear negative relationship between wood density and cavitation threshold across six *Nothofagus* species from Argentina and Chile including *N. dombeyi* (Bucci et al. 2012) which indicates that a change in wood density from 0.50 to 0.54 g cm^{-3} results in a 0.7 MPa more negative stem P_{50}.

Stomatal conductance and leaf turgor loss point

Previous studies have showed a differential stomatal response to drought for these study species. While *N. dombeyi* exhibits increase in stomatal conductance during the dry season and at midday when the atmospheric demand is high (Zúñiga et al. 2006; Jiménez-Castillo et al. 2011), *A chilensis* shows an early stomatal closure in response to moderate air saturation deficits even when soil water content is not limiting (Gyenge et al. 2007). This differential behavior to drought is also common in Mediterranean conifers species and angiosperms (Martínez-Ferri et al. 2000; Poyatos et al. 2013). Although in this study stomatal conductance was not measured, a tight stomatal

control in *A. chilensis* can be inferred from sap flow patterns, which exhibited a rapid decline after reaching its maximum value. For other South American *Nothofagus* species (*N. pumilio* and *N. antarctica*) Pfautsch et al. (2014) found, also using sap flow data, that stomatal regulation of transpiration is low in these species because tree water use increased linearly with increasing air saturation deficits. Stomatal control observed in *A. chilensis*, which was not sufficient to avoid turgor loss, has the cost of reduced carbon gains but the benefit of maintaining relatively high water potentials and to reduce the possibility that plant reaches the true threshold of irreversible drought damage.

Leaf and stem capacitance

Leaf tissues can act as water storage compartments (Sack et al. 2003) which may release water to the transpiration stream to buffer rapid changes in leaf water potentials (Hao et al. 2008). Consistent with our results (higher leaf capacitance in *A. chilensis*) Brodribb et al. (2005) found that conifers from Chilean forests including *A. chilensis* exhibit substantial capacitance with small shoots able to function for long periods (from 10 min in *A. chilensis* to 108 min in *Araucaria araucana*) without hydraulic connections to the rest of the plant. Despite having high leaf capacitance, leaves of *A. chilensis* lose cell turgor. The substantial water release from internal water storage after turgor loss point as observed in *A. chilensis* could help to slow the rate of leaf hydraulic conductance loss at leaf water potentials close to P_{88} and to contribute to the large safety margin observed in this species.

Large leaf and sapwood capacitance in *A. chilensis* is consistent with the diurnal dynamic of stem diameter contraction and expansion, and with the kinetics of crown and basal sap flow patterns indicating that a substantial amount of water is released from stem water storages (19.3 % of the total daily water use). Although we did not measure sap flow in *N. dombeyi*, some studies indicate a positive relation between water stored use estimated from sap flow measured at different tree height and sapwood capacitance (Scholz et al. 2007) across several tree species, suggesting that *N. dombeyi* may have less water use from internal storages due to its lower capacitance and saturated water content. In addition, functional relationships between sapwood density and capacitance, and sapwood density and saturated water content found for tree species in other ecosystems indicate that a small increase in wood density such as the one observed in *N. dombeyi* respect to *A. chilensis*, leads to a decrease of 15–30 % in terms of capacitance (Scholz et al. 2007; Meinzer et al. 2008) and

23 % in the water stored; thus the amount of water released into the xylem stream to buffer the water potential decline may be lower in *N, dombeyi*. On the other hand, the cortex (bark parenchyma tissue) can serve as water source as reflected by the diurnal variations in the stem diameter (cortex + sapwood) and in the sapwood. The dynamics in the contraction and expansion of both tissues suggest a water movement from the living cortex tissues to the sapwood driven by a water potential gradient favoring radial water movement. Capacitive release of water is an important aspect of plant hydraulics which is instrumental to preserve the long-distance water transport and to help avoid stem hydraulic dysfunction (Scholz et al. 2007; McCulloh et al. 2013).

In conclusion we observed that *A. chilensis* exhibit different physiological mechanisms to maintain the water potential far from its hydraulic functional limit (P_{88}) such as high hydraulic capacitance of the leaves and stems, high stored water use, ability to recover hydraulic conductivity and tight stomatal control of evaporative losses to alleviate the drought effects during years with anomalously low rainfall. Strong hydraulic segmentation in *N. dombeyi* does not have an adaptive value to survive during severe droughts. Higher vulnerability to cavitation in leaves than in stems result in leaf dehydration followed by leaf abscission when leaf water potential strongly decline due to water stress, which may lead to carbon starvation. The loss of gas exchange surface during drought summers in *N. dombeyi* may reduce carbohydrate production and storage required to avoid freezing injury in the following winter. Although other causes such as leaf overheating could be involved in the lack of survival behavior, die-back in *N. dombeyi* likely occurs due to a combination of leaf hydraulic failure during long droughts together with carbon starvation that result in carbohydrate source limitation. The results obtained in this study are of importance for predicting long term responses (forest structure and demography) to droughts, which are expected to increase in the next 50 years in the western slopes of the southern Andes (Collins et al. 2013).

References

Adams HD, Germino MJ, Breshears DD, Barron-Gafford GA, Guardiola-Claramonte M, Zou CB, Huxman TE (2013) Non-structural leaf carbohydrate dynamics of *Pinus edulis* during drought-induced tree mortality reveal role for carbon metabolism in mortality mechanism. New Phytol 197(1142):1151. doi:10.1111/nph.12102

Alberdi M (1987) Ecofisiología de especies chilenas del género. Nothofagus Bosque 8:77–84

Allen C, Alison K, Chenchouni H, Bachelet D, McDowell N, Vennetier M, Kitzberger T, Rigling A, Breshears D, Hogg E, Gonzalez P, Fensham R, Zhang Z, Castro J, Demidova N, Lim J, Allard G, Running S, Semerci A, Cobb B (2010) A global overview of drought and heat-induced tree mortality reveals emerging change risks for forests. Forest Ecol Manage 259:660–684

Allen CD, Macalady AK, Chenchouni H, Bachelet D, McDowell N, Vennetier M, Kitzberger T, Rigling A, Anderegg WRL, Berry JA, Smith DD, Sperry JS, Anderegg LDL, Field CB (2012) The roles of hydraulic and carbon stress in a widespread climate-induced forest die-off. Proc Natl Acad Sci USA 109:233–237

Barigah ST, Charrier O, Douris M, Bonhomme M, Herbette S, Ameglio T, Fichot R, Brignolas F, Cochard H (2013) Water stress-induced xylem hydraulic failure is a causal factor of tree mortality in beech and poplar. Ann Bot 112:1431–1437

Barnard DM, Meinzer FC, Lachenbruch B, McCulloh KA, Johnson DM, Woodruff DR (2011) Climate-related trends in sapwood biophysical properties in two conifers: avoidance of hydraulic dysfunction through coordinated adjustments in xylem efficiency, safety and capacitance. Plant Cell Environ 34:643–654

Blackman CJ, Brodribb TJ, Jordan GJ (2009) Leaf hydraulics and drought stress: response, recovery and survivorship in four woody temperate plant species. Plant Cell Environ 32:1584–1595

Breshears DD, Cobb NS, Rich PM, Price KP, Allen CD, Balice RG, Romme WH, Kastens JH, Floyd ML, Belnap J et al (2005) Regional vegetation die-off in response to global-change-type drought. Proc Natl Acad Sci USA 102:15144–15148

Brodribb TJ, Cochard H (2009) Hydraulic failure defines the recovery and point of death in water-stressed conifers. Plant Physiol 149:575–584

Brodribb TJ, Holbrook NM (2003) Stomatal closure during leaf dehydration correlation with other leaf physiological traits. Plant Physiol 132:2166–2173

Brodribb TJ, Holbrook NM, Zwieniecki MA, Palma B (2005) Leaf hydraulic capacity in ferns, conifers and angiosperms: impacts on photosynthetic maxima. New Phytol 165:839–846

Brodribb TJ, Bowman DJMS, Nichols S, Delzon S, Burlett R (2010) Xylem function and growth rate interact to determine recovery rates after exposure to extreme water deficit. New Phytol 188:533–542

Bucci SJ, Scholz FG, Goldstein G, Meinzer FC, Sternberg SL (2003) Dynamic changes in hydraulic conductivity in petioles of two savannas tree species: factors and mechanisms contributing to the refilling to embolized vessels. Plant Cell Environ 26:1633–1645

Bucci SJ, Scholz FG, Goldstein G, Meinzer FC, Franco AC, Zhang Y, Hao G-Y (2008) Water relations and hydraulic architecture in Cerrado trees: adjustments to seasonal changes in water availability and evaporative demand. Braz J Plant Physiol 20:233–245

Bucci SJ, Scholz FG, Campanello PI, Montti L, Jimenez M, La Manna L, Rockwell A, Guerra P, Lopez-Bernal P, Troncoso O, Holbrook MN, Goldsein G (2012) Hydraulic differences along the water transport system of South American Nothofagus species: do leaves protect the stem functionality? Tree Physiol 32:880–892

Bucci SJ, Scholz FG, Peschiutta ML, Arias N, Meinzer FC, Goldstein G (2013) The stem xylem of Patagonian shrubs operates far from the point of catastrophic dysfunction and is additionally protected from drought- induced embolism by leaves and roots. Plant Cell Environ 36:2163–2174

Carnicer J, Barbeta A, Sperlich D, Coll M, Peñuelas J (2013) Contrasting trait syndromes in angiosperms and conifers are associated with different responses of tree growth to temperature on a large scale. Front Plant Sci 4:409. doi:10.3389/fpls.2013.00409

Choat B, Jansen S, Brodribb TJ, Cochard H, Delzon S, Bhaskar R, Bucci SJ, Feild TS, Gleason SM, Jacobsen AL, Lens F, Maherali H, Martinez-Vilalta J, Mayr S, Mencuccini M, Mitchell PJ, Nardini A, Pittermann J, Pratt RB, Sperry JS, Westoby M, Wright IJ, Zanne A (2012) Global convergence in the vulnerability of forests to drought. Nature 491:752–756

Coll M, Peñuelas J, Ninyerola M, Pons X, Carnicer J (2013) Multivariate effect gradients driving forest demographic responses in the Iberian Peninsula. For Ecol Manage 303:195–209

Collins M, Knutti R, Arblaster J, Dufresne J-L, Fichefet T, Friedlingstein P, Gao X, Gutowski WJ, Johns T, Krinner G, Shongwe M, Tebaldi C, Weaver AJ, Wehner M (2013) Long-term climate change: projections, commitments and irreversibility. In: Stocker TF, Qin D, Plattner G-K, Tignor M, Allen SK, Boschung J, Nauels A, Xia Y, Bex V, Midgley PM (eds) Climate change 2013: the physical science basis, Contribution of working group I to the fifth assessment report of the Intergovernmental Panel on climate change. Cambridge University Press, New York

Do F, Rocheteau A (2002) Influence of natural temperature gradients on measurements of xylem sap flow with thermal dissipation probes. 2. Advantages and calibration of a noncontinuous heating system. Tree Physiol 22:649–654

Domec J-C, Gartner BL (2001) Cavitation and water storage capacity in bole xylem segments of mature and young Douglas-®r trees. Trees 15:204–214

Fajardo A, Piper FI, Hoch G (2013) Similar variation in carbon storage between deciduous and evergreen treeline species across elevational gradients. Ann Bot 112:623–631

Goldstein G, Andrade JL, Meinzer FC, Holbrook NM, Cavelier J, Jackson P, Celis A (1998) Stem water storage and diurnal patterns of water use in tropical forest canopy trees. Plant, Cell Environ 21:397–406

Gómez-Aparicio L, Garcia Valdes R, Ruiz-Benito P, Zavala MA (2011) Disentangling the relative importance of climate, size and competition on tree growth in Iberian forests: implications for forest management under global change. Glob Change Biol 17:2400–2414

Granier A (1985) Une nouvelle méthode pour la mesure du flux de séve brute dans le tronc des arbres. Ann Sci For 42:193–200

Granier A (1987) Evaluation of transpiration in a Douglas fir stand by means of sap flow measurement. Tree Physiol 3:309–320

Greslebin AG, Hansen EM, Winton L, Rajchenberg M (2005) Phytophthora species from declining *Austrocedrus chilensis* forests in Patagonia, Argentina. Mycologia 97:218–228

Gyenge JE, Fernández ME, Schlichter T (2007) Influence of radiation and drought on gas exchange of *Austrocedrus chilensis* seedlings. BOSQUE 28:220–225

Hacke UG, Sperry JS, Pockman WT, Davis SD, McCulloh K (2001) Trends in wood density and structure are linked to prevention of xylem implosion by negative pressure. Oecologia 126:457–461

Hao G-W, Hoffmann WA, Scholz FG, Bucci SJ, Meinzer FC, Franco AC, Cao K-F, Goldstein G (2008) Stem and leaf hydraulics of congeneric tree species from adjacent tropical savanna and forest ecosystems. Oecologia 155:405–415

Hartmann H, Ziegler W, Kolle O, Trumbore S (2013) Thirst beats hunger declining hydration during drought prevents carbon starvation in Norway spruce saplings. New Phytol 200:340–349

Jiménez-Castillo M, Lobos-Catalán P, Aguilera-Betti I, Rivera R (2011) Tasas diarias de transpiración y relaciones hídricas en especies arbóreas con distinto nivel de sombra tolerancia en un bosque templado chileno. Gayana Botánica 68:155–162

Johnson DM, Woodruff DR, McCulloh KA, Meinzer FC (2009) Leaf hydraulic conductance, measured in situ, declines and recovers daily: leaf hydraulics, water potential and stomatal conductance in four temperate and three tropical tree species. Tree Physiol 29:879–887

Johnson DM, McCulloh KA, Meinzer FC, Woodruff DR (2011) Hydraulic patterns and safety margins, from stem to stomata, in three eastern US tree species. Tree Physiol 31:659–668

La Manna L, Rajchenberg M (2004) The decline of *Austrocedrus chilensis* forests in Patagonia, Argentina: soil features as predisposing factors. For Ecol Manage 190:345–357

Larjavaara M, Muller-Landau HC (2010) Rethinking the value of high wood density. Funct Ecol 24:701–705

Martínez-Ferri E, Balaguer L, Valladares F, Chico JM, Manrique E (2000) Energy dissipation in drought-avoiding and drought-tolerant tree species at midday during the Mediterranean summer. Tree Physiol 20:131–138

McCulloh KA, Johnson D, Meinzer FC, Woodruff DR (2013) The dynamic pipeline: hydraulic capacitance and xylem hydraulic safety in four tall conifer species Plant Cell Environ doi: 10.1111/pce.12225

McDowell N, Pockman WT, Allen CD, Breshears DD, Cobb N, Kolb T, Plaut J, Sperry J, West A, Williams DG et al (2008) Mechanisms of plant survival and mortality during drought: why do some plants survive while others succumb to drought? New Phytol 178:719–739

McDowell NG, Beerling DJ, Breshears DD, Fisher RA, Raffa KF, Stitt M (2011) The interdependence of mechanisms underlying climate-driven vegetation mortality. Trends Ecol Evol 26:523–532

Meinzer FC, James SA, Goldstein G, Woodruff DR (2003) Whole-tree water transport scales with sapwood capacitance in tropical forest canopy trees. Plant Cell Environ 26:1147–1155

Meinzer FC, Johnson DM, Lachenbruch B, McCulloh KA, Woodruff DR (2009) Xylem hydraulic safety margins in woody plants: coordination of stomatal control of xylem tension with hydraulic capacitance. Funct Ecol 23:922–930

Mundo IA, El Mujtar VA, Perdomo MH, Gallo LA, Villalba R, Barrera MD (2010) *Austrocedrus chilensis* growth decline in relation to drought events in Northern Patagonia, Argentina. Trees 24:561–570

Nardini A, Lo Gullo MA, Salleo S (2011) Refilling embolized xylem conduits: is it a matter of phloem unloading? Plant Sci 180:604–611

Pfautsch S, Peri PL, Macfarlane C, van Ogtrop F, Adams MA (2014) Relating water use to morphology and environment of *Nothofagus* from the world's most southern forests. Trees 28:125–136

Plaut JA, Wadsworth WD, Pangle R, Yepez EA, McDowell NG, Pockman WT (2013) Reduced transpiration response to precipitation pulses precedes mortality in a pinon–juniper woodland subject to prolonged drought. New Phytol 200:375–387

Poyatos R, Aguade D, Galiano L, Mencuccini M, Martınez-Vilalta J (2013) Drought-induced defoliation and long periods of near-zero gas exchange play a key role in accentuating metabolic decline of Scots pine. New Phytol 200:388–401

Pratt RB, Jacobsen A, Ewers FW, Davis SD (2007) Relationships among xylem transport, biomechanics and storage in stems and roots of nine Rhamnaceae species of the California chaparral. New Phytol 174:787–798

Reyes-Díaz M, Alberdi M, Piper F, Bravo LA, Corcuera LJ (2005) Low temperature responses of *Nothofagus dombeyi* and *Nothofagus nitida*, two evergreen species from south central Chile. Tree Physiol 25:1389–1398

Richards AE, Wright IJ, Lenz TI, Zanne AE (2013) Sapwood capacitance is greater in evergreen sclerophyll species growing in high compared to low-rainfall environments. Funct Ecol doi: 10.1111/1365-2435.12193

Riveros M, Perez M, Baez P, Baez A (2003) Resource allocation dynamics preceding flowering in species of the genus Nothofagus. Bosque 24:85–95

Sack L, Cowan PD, Jaikumar N, Holbrook NM (2003) The 'hydrology' of leaves: co-ordination of structure and function in temperate woody species. Plant Cell Environ 26:1343–1356

Sala A, Piper F, Hoch G (2010) Physiological mechanisms of drought-induced tree mortality are far from being resolved. New Phytol 186:274–281

Sala A, Woodruff DR, Meinzer FC (2012) Carbon dynamics in trees: feast or famine? Tree Physiol 32:764–775

Scholz FG, Bucci SJ, Goldstein G, Meinzer FC, Franco AC, Miralles-Wilhelm F (2007) Biophysical properties and functional significance of stem water storage tissues in neo-tropical savanna trees. Plant Cell Environ 30:236–248

Scholz FG, Bucci SJ, Goldstein G, Meinzer FC, Franco AC, Salazar A (2008) Plant-and Stand level variation in biophysical and physiological traits along tree density gradients in the Cerrado. Braz J Plant Physiol 20:217–232

Scholz FG, Phillips NG, Bucci SJ, Meinzer FC, Goldstein G (2011) Hydraulic capacitance. In: Meinzer FC et al. (eds) Biophysics and functional significance of internal water sources in relation to tree size in size- and age-related changes in tree structure and function Vol. 4 Springer 341–361

Suarez ML, Kitzberger T (2008) Recruitment patterns following a severe drought: long-term compositional shifts in Patagonian forests. Can J For Res 38:3002–3010

Suarez ML, Kitzberger T (2010) Differential effects of climate variability on forest dynamics along a precipitation gradient in northern Patagonia. J Ecol 98:1023–1034

Suarez ML, Ghermandi L, Kitzberger T (2004) Factors predisposing episodic drought-induced tree mortality in *Nothofagus*: site, climatic sensitivity and growth trends. J Ecol 92:954–966

Tyree MT, Ewers FW (1991) The hydraulic architecture of trees and other woody plants. New Phytol 119:345–360

Tyree MT, Sperry JS (1989) Vulnerability of xylem to cavitation and embolism. Annu Rev Plant Phys Mol Bio 40:19–38

Urli M, Porte AJ, Cochard H, Guengant Y, Burlett R, Delzon S (2013) Xylem embolism threshold for catastrophic hydraulic failure in angiosperm trees. Tree Physiol 33:672–683

Velez ML, Silva PV, Troncoso OA, Greslebin AG (2012) Alteration of physiological parameters of *Austrocedrus chilensis* by the pathogen *Phytophthora austrocedrae*. Plant Physiol 61:877–888

Wheeler JK, Huggett BA, Tofte AN, Rockwell FE, Holbrook NM (2013) Cutting xylem under tension or supersaturated with gas can generate PLC and the appearance of rapid recovery from embolism. Plant Cell Environ 36:1938–1949

Zúñiga R, Alberdi M, Reyes-Díaz M, Olivares O, Hess S, Bravo LA, Corcuera LJ (2006) Seasonal changes in the photosynthetic performance of two evergreen Nothofagus species in south central Chile. Revista Chilena de Historia Natural 79:489–504

Zwieniecki MA, Holbrook NM (1998) Short term changes in xylem water conductivity in white ash, red maple and Sitka spruce. Plant Cell Environ 21:1173–1180

Zwieniecki MA, Holbrook MN (2009) Confronting Maxwell's demon: biophysics of xylem embolism repair. Trends Plant Sci 14:530–534

Zwieniecki MA, Brodribb TJ, Holbrook MN (2007) Hydraulic design of leaves: insights from rehydration kinetics. Plant Cell Environ 30:910–921